DARPA YFA Final Report
Grant # N66001-09-1-2091
October 1, 2009 - September 6, 2012

Georgia Institute of Technology

Technical Point of Contact: Dr. Baratunde Cola

Administrative Point of Contact: Mr. Dan Sibble

Photo-Thermal Enhanced Carbon Nanotube Rectenna Arrays for Solar Energy Conversion

Technical Area: *Power and Energy*

DARPA Mentor: Dr. Nibir Dhar

Title: PHOTOTHERMAL ENHANCED CARBON NANOTUBE RECTENNA ARRAYS FOR SOLAR ENERGY

Grant Number: N66001-09-1-2091

Reporting Year: Final Report (2009-2012)

Introduction

The inherent advantages of direct energy conversion have motivated researchers for many decades, yet a suitable technology that offers a favorable combination of high thermodynamic efficiency and capacity has not emerged. An intuitive extension of microwave theory to IR and optical frequencies reveals an appealing solution to this dilemma that involves the use of small-scale antennas coupled to diodes (*i.e.* rectennas) that convert AC signals received from the solar electromagnetic field directly to DC power. Theoretically, rectenna-based power conversion can be executed with efficiencies that approach 100% [1] – the conversion efficiency is not Carnot limited like thermoelectrics or quantum limited like photovoltaics. For example, rectennas used for microwave power conversion, first demonstrated by Raytheon in the 1960s, have achieved efficiencies greater than 85% [2]. However, to achieve such high efficiencies with solar conversion will require improved antenna materials for efficient coupling to IR and optical wavelengths and low capacitance diodes with improved nonlinearity and asymmetry that, to date, have not been realized [3-5].

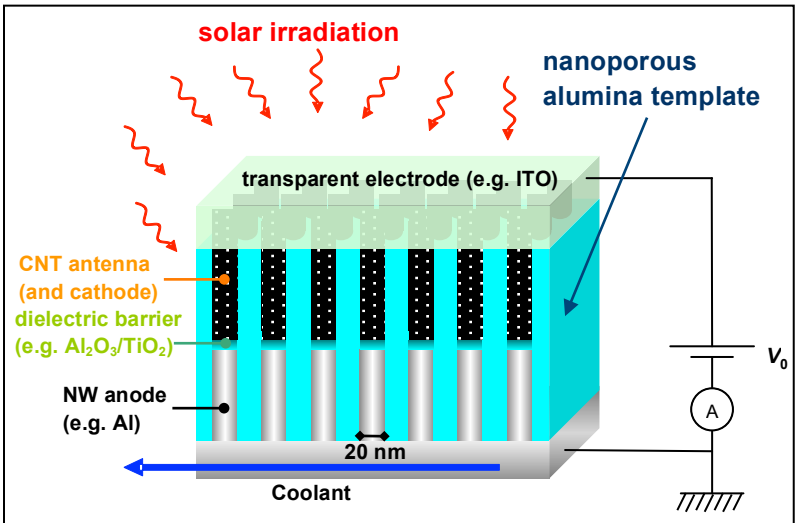

Figure 1. Conceptual solar energy conversion device with a dense array of CNT-based rectennas. CNTs couple to the solar electromagnetic field and the CNT-insulator-NW diode junction with photothermal enhanced electron emission efficiently converts the induced THz signals to DC power.

The emergence of nanomaterials offers significant promise in alleviating these limitations. In particular, carbon nanotubes (CNTs) have been shown to provide exceptional

functional performance in nanoelectronics and sensing applications, yet numerous challenges remain both in fundamental understanding of their transport physics and in achieving scalable and robust manufacturing methods for integrated devices. In this work, we develop a CNT-based rectenna device for direct solar energy conversion that exploits intrinsically small device contacts, which enable low diode capacitance, and demonstrated antenna coupling to solar wavelengths [6] and ultra-low electron scattering rates via quantum-confined transport that could facilitate substantial improvements in thermodynamic capacity and efficiency. The CNTs are developed to efficiently couple to the solar electromagnetic field, conduct electrons with low scattering rates to the diode junction, and emit electrons toward a low-work-function anode (see Figure 1). Because they also absorb solar irradiation via photon-electron-phonon energy exchange, enhanced electron emission toward the anode, which improves diode efficiency and capacity, could be promoted by *synergistic* photonic and thermal excitation in the CNTs. In contrast to traditional photovoltaic devices, which are quantum systems limited by material bandgaps, antennas offer a more efficient and tunable direct solar conversion mechanism that relies on natural resonance and bandwidth of operation as a function of physical antenna geometry.

This research program therefore seeks to enhance the combined effects of solar-derived electromagnetic, thermal, and photonic electron excitation in order to create devices with improved power generation capacity and efficiency as compared to conventional direct energy conversion technologies. Simple theory, in which an ideal antenna receiver is represented by an AC voltage source $V \cdot \cos(\omega \cdot t)$ at solar frequency ω with an internal real impedance R_A, suggests that the maximum power delivered to the diode component of the rectenna is inversely proportional to $\omega \cdot C_D \cdot R_A$ (C_D is the diode capacitance) for $\omega \cdot C_D \cdot R_A >> 1$, and equal to the incident power P ($= V^2/8 \cdot R_A$) when $\omega \cdot C_D \cdot R_A << 1$ [1]. These conditions illustrate that sufficiently low diode capacitance and antenna impedance facilitates conversion of the entire solar spectrum (from approximately 150 to 1000 THz) to DC power. The generated capacity and efficiency of this converted power are strong functions of the rectified diode current, which, in the device developed here, is anticipated to be enhanced by the establishment of 'hot' electrons in the CNTs that tunnel with increased probability through the quasi one-dimensional (1D) diode system (tunneling probability increases with electron momentum normal to the barrier [7]). The

realization of such a device in the past has been hindered by many factors, including the difficulty in reproducibly fabricating stable point-contact tunnel diodes and nanoscale antenna with desired characteristics, and the inability to sustain 'hot' carrier ensembles under high background temperatures because of non-radiative recombination.

Technical Accomplishments

Technical Objectives

This project was aimed at fabricating dense ordered arrays of vertical carbon nanotube (CNT) rectenna with diode components exhibiting high asymmetry and nonlinearity. Our broad objectives were to explore and demonstrate the devices with solar energy conversion at high solar frequencies and with efficient power conversion that can be used in a variety of defense applications.

Technical Approach

Our approach was to fabricate, characterize, and to understand the physical processes in order to achieve high rectification in the diode component of CNT rectenna. Our research focused on understanding the various aspects of these novel device structures that can be used in a variety of promising applications such as switching diode, optical rectenna for energy harvesting, and infrared photodectors. Device fabrication, scanning electron microscopy (SEM) studies, work function measurements and electrical characterization of the large number of fabricated devices was preformed in this program. We concluded the program with a demonstration of rectenna solar energy conversion using the vertical CNT devices.

Early Efforts

Numerous fabrication challenges defined our early efforts to create CNT rectenna devices. The following is a brief summary of efforts and challenges in the first 2 years of this program. The first approach to fabrication of CNT rectenna arrays included in-house fabrication of porous anodic alumina (PAA) templates, which were to be used for CNT growth and device fabrication within. The goal was to create PAA with pore sizes on the order of 20 nm. Many recipes were tried, but none could be developed to produce templates with consistent properties

such as pore order and size, and low number of pore defects. PAA was fabricated on silicon substrates. We had issues with delamination of the few successful PAA templates after CNT growth in the templates. CNT growth in the templates was another challenge. Because of the small target pore diameters, the deposition of catalyst metal for CNT growth was difficult. This deposition occurred using an electrochemical deposition process. It was difficult to control the deposition rate such that uniform nickel or iron CNT catalyst deposition occurred in all, or even a majority of the template pores. Electrodeposition of aluminum as a low workfunction metal was attempted in parallel with attempts to fabrication PAA templates. This effort was not successful do the challenges that resulted from the need to deposit the aluminum in an inert atmosphere. Moisture and air exposure likely prevented desired deposition despite the use of a glove box and/or nitrogen purging of the deposition electrolyte during the process. The limited success of early efforts included the development of a reasonably consistent recipe for the fabrication of PAA templates with diameters of 60 nm, which was 3-fold larger than the desired pore diameter. In this template, we were able to fabricate CNT-nickel nanowire composites and nickel-alumina-nickel diode structures. The CNT-nickel nanowire samples were measured with an electrically conductive atomic force microscope (AFM) tip and the response was ohmic. We were not able to measure the electrical response of the nickel-alumina-nickel structures because inconsistent pore filling made locating a single junction with the AFM difficult. The challenges of our early efforts lead to a period of brainstorming that produced a pivot to a more successful approach, which is discussed below.

Efforts after The Pivot

After the pivot, we accomplished the following: **(i)** We optimized and compared the CNT growth by low-pressure chemical vapor deposition (LPCVD) on medium resistivity (0.01-0.05 Ω.cm) and low resistivity Si wafers (0.001-0.005 Ω.cm). The work function measurements of the CNTs by Kelvin Probe provided an understanding of the basic diode operation principles and the correlation of the observed asymmetry and non-linearity in the current-voltage (*I-V*) characteristics. **(ii)** We developed carbon nanotube-oxide-metal (CNT-O-M) vertical diode arrays structures by depositing alumina via atomic layer deposition (ALD) followed by the top contact metal. **(iii)** We demonstrated the influence of varying the work function of the top metal electrode on the electrical performance of the CNT-O-M diodes to identify the champion diodes

with high rectification ratio. The use of low work function metal such as Ca showed superior diode characteristics with higher asymmetry in the *I-V* curve in comparison to a higher work function metal such as Al. **(iv)** We also demonstrated that the fabricated CNT-O-M diodes show excellent electrical stability in the temperature ranging from 5-77 ˚C. **(v)** Finally, we demonstrated significant light response and harvesting with the CNT-O-M rectenna arrays.

A. Fabrication of Carbon Nanotube-Oxide-Metal Vertical Diode Arrays (CNT Rectenna)

Vertically aligned arrays of CNTs were grown on single crystal Si substrates diced into 1x1 inch substrates. Ti, Al, Fe films in thicknesses of 100, 10, 3 nm were evaporated onto the Si as support and catalyst layers for CNT growth. Afterwards the CNTs were grown using a low-pressure chemical vapor deposition (LPCVD) process, 850 °C and 1 kPa, in an Aixtron Black Magic© reactor with C_2H_2 as the carbon source gas. The growth time was optimized to be 3 minute to grow CNTs with average height of 5-8 microns. A conformable coating of alumina (8 nm), the dielectric layer for the rectenna devices, is deposited on outside of CNTs by ALD at 250 °C using trimethylaluminum (TMA) vapor. In order to make TMA and H_2O vapor effectively diffuse into CNT array, large exposure of TMA and H_2O are used for each ALD cycle. To oxidize the uncoated CNTs left during first set of cycles, we used plasma etching for 5 minutes in between of two sets of ALD cycles. A metal top contact of Al/Ca was then deposited on the array to form the device. A scanning electron micrograph (SEM) of a representative CNT-oxide-metal device and the schematic view of the representative device are shown in Figure 2.

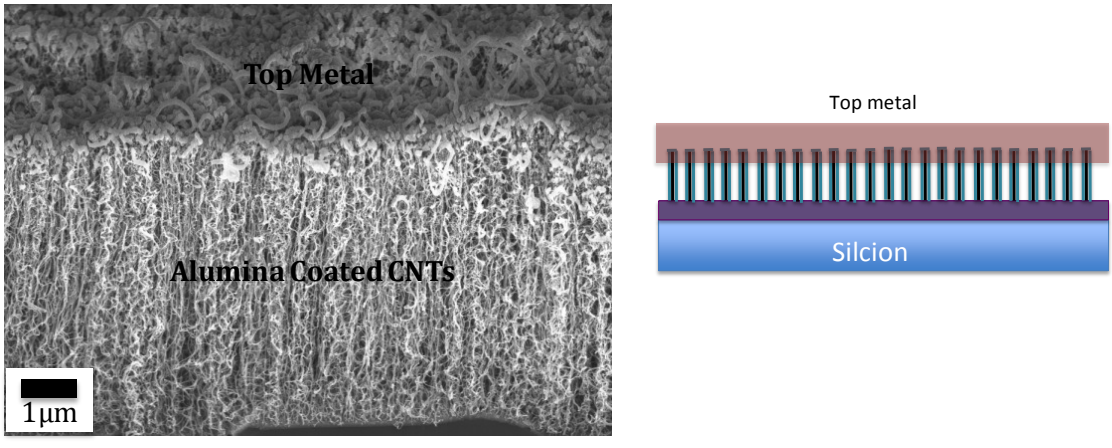

Figure 2. Scanning electron micrograph and the representative schematic of CNT-oxide-metal device.

B. Electrical Characteristics of Carbon Nanotube-Oxide-Metal Vertical Diode Arrays (CNT Rectenna)

The current voltage (*I-V*) characteristics measured for three different devices using Ca top electrode and an effective area of 0.01 cm^2 (effective area described by the top metal electrode) are shown in Figure 3 (a) ((b) shows the semi logarithmic plot of the data). Figure 3 (c) shows the picture of the actual devices fabricated on 1"x1" sample with two different areas as defined by the top metal electrode.

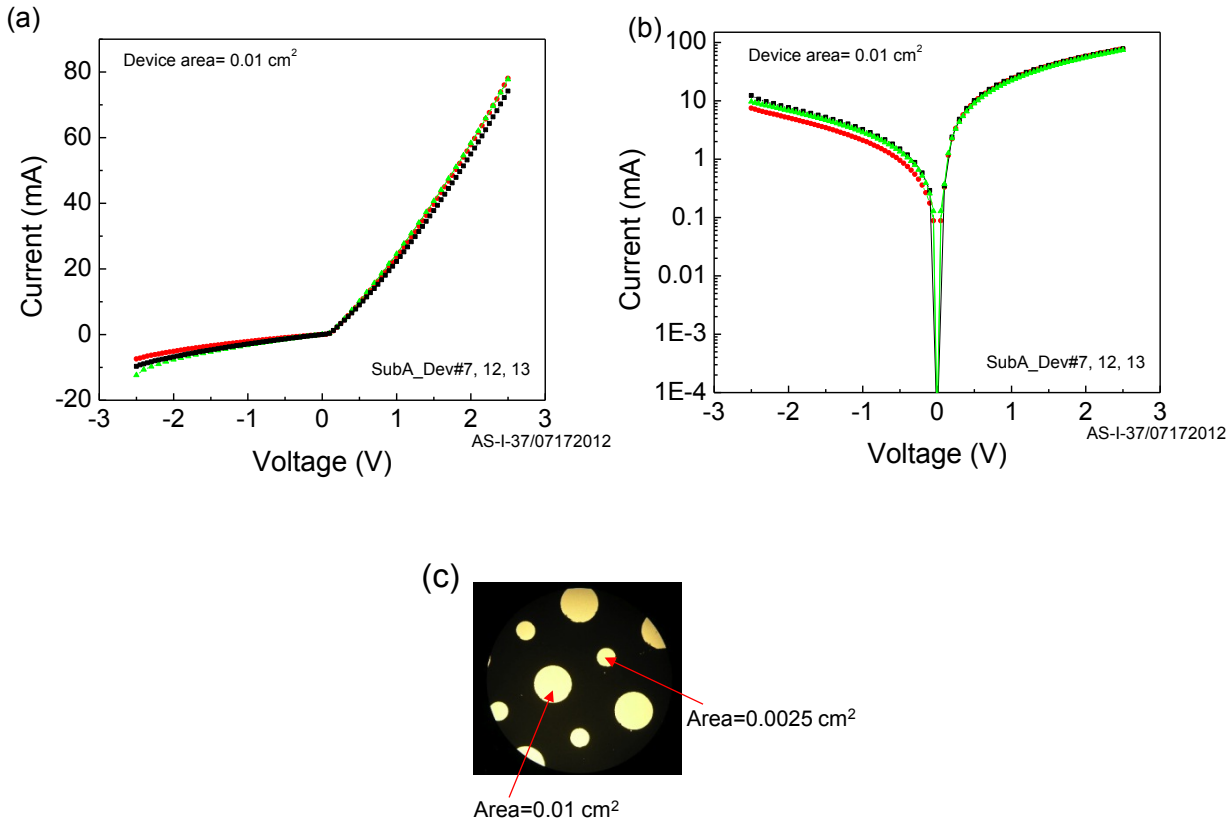

Figure 3. (a) Current-voltage (*I-V*) characteristics of CNT-O-M vertical diode array devices, (b) shows the semi logarithmic plots of the data shown in (a), and (c) shows the optical image of the fabricated devices (area defined by the top metal).

It can be seen from Figure 3 that *I-V* characteristics of the fabricated CNT-O-M devices show reproducibility from device to device. Additionally, the devices were stable during the multiple scans (see Figure 4) demonstrating the operational stability of these diodes. These results indicate that our approach of fabricating the vertical arrays of CNT-O-M tunneling diodes

is very promising for large area fabrication when compared with other metal-oxide–metal rectifying tunnel devices that require expensive, time consuming, and challenging fabrication techniques, *e.g.*, e-beam nanolithography.

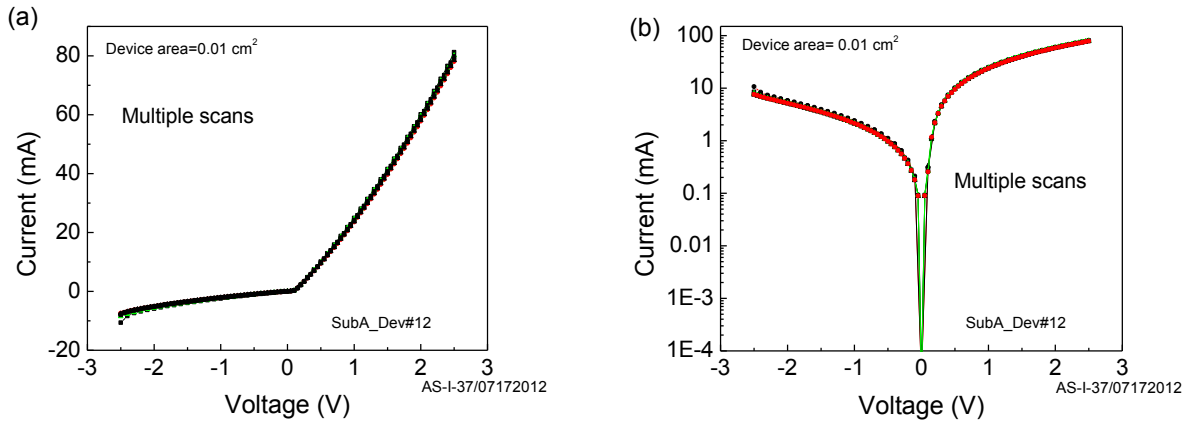

Figure 4. (a) Current-voltage (*I-V*) characteristics of CNT-O-M vertical diode array devices during multiple scans (demonstrating the operational stability), and (b) shows the semi logarithmic plot the data shown in (a).

C. Effect of Top Electrode Metal Work Function on Diode rectification

In order to understand the basic tunneling physics mechanism in the CNT-O-M diode array devices and to correlate the effect of using the low work function metals, we fabricated several devices in the same batch with similar CNT heights and 8 nm of Al_2O_3 deposited by ALD in the same run followed by different top metal electrodes. For top metal electrode, either aluminum (Al, work function ~ 4.3 eV) or calcium (Ca, work function ~ 2.9 eV) was chosen as a case study on large number of devices fabricated on different substrates and in different batches.

Figure 5 compares the electrical characteristics of several devices using Ca or Al top electrodes. The results are shown for two different device areas (0.01 cm^2, and 0.0025 cm^2) as defined by the top electrode (see optical picture in Fig. 3 (c)). These results on multiple devices show a higher rectification for Ca electrode based CNT-O-M devices than in the case of Al based devices. Therefore, by selecting the electrode metal with more difference in the work function with respect to CNT work function will provide a tunneling current with higher asymmetry with respect to the voltage applied across the CNT-O-M diode, and will lead to the potential for excellent rectification.

In order to understand and correlate these electrical characteristics with the metal work function, a representative potential energy level diagram that considers a basic mechanism of a typical metal-insulator-metals (MIM) tunneling diode is shown in Figure 5 (c). When two metals with different work functions (CNTs and top metal) make contact with a thin insulating oxide, a net electron flow will take place until the Fermi level for the two metals gets aligned and an equilibrium state is reached as shown in the energy level diagram (contact state). Considering the case for an Al top electrode, when a negative voltage is applied to the Al with respect to CNTs the effective barrier height for the electron flow from Al toward CNTs will be reduced and a net flow of current will be seen (see forward bias current). By contrast, upon applying a positive bias to the low work function metal (Al in this case) will raise the effective barrier height for the electron flow (reverse bias conditions). The influence of the effective barrier height on the net flow of current due to the applied bias is assumed at the onset of Fowler-Nordheim (FN) tunneling. The probability of FN tunneling is exponentially dependent upon the insulator thickness and the effective barrier height at the electrode/insulator interface. Thus, for a fixed insulator thickness, using a lower work function top metal electrode such as Ca (see Figure 5 (a) and (b)) will have relatively lower barrier height at the interface, and the magnitude of the FN tunneling currents should be larger at larger biases in the forward bias conditions. The higher the difference between the work function values of the CNTs and the top metal electrode, the higher the asymmetry in the observed current and the rectification ratio from the DC current-voltage measurements.

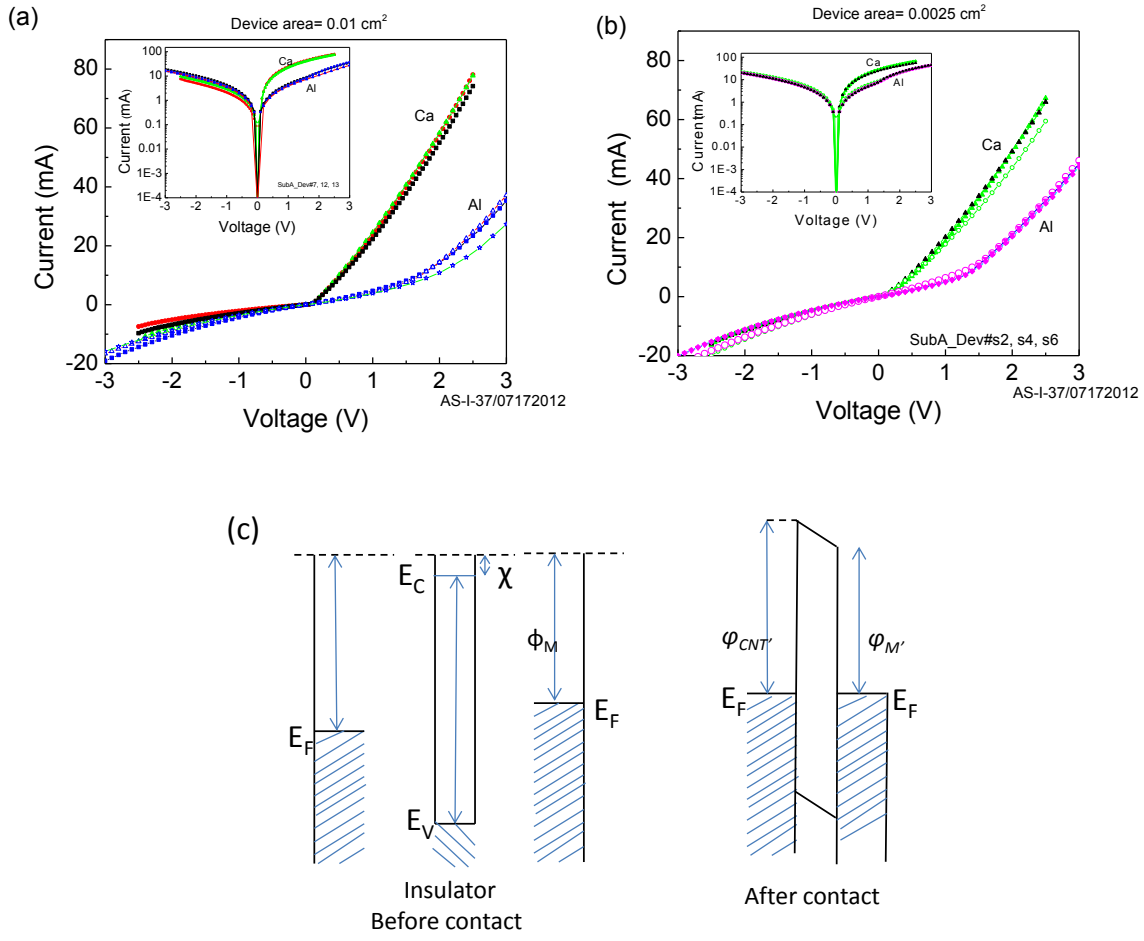

Figure 5. (a) Comparison of the current-voltage (*I-V*) characteristics of CNT-O-M vertical diode array devices using lower work function metal (Ca, 2.9 eV) and higher work function metal (Al, 4.3 eV) top electrodes, (b) shows the results for smaller area (0.0025 cm^2) devices, and (c) represents an equilibrium potential energy level diagram with an asymmetric tunnel diode.

D. Effect of CNT Work Function on Diode rectification

To investigate and study the influence of the work function of the CNTs, which can exhibit different values depending upon the growth conditions, substrates etc., we measured the work function values of the CNTs on the substrates with different resistivity values (see Figure 6 (a)). The work function values were measured using a Kelvin probe (Besocke Delta Phi) on three different spots on the same sample, and the CNTs grown in different batches also. A highly ordered pyrolytic graphite (HOPG) crystal was used as a reference sample. The comparison of

the work function values for the CNTs that were grown on medium resistivity (0.01-0.05 Ω.cm) Si exhibited higher values when compared to that of the CNTs that were grown on low resistivity Si wafers (0.001-0.005 Ω.cm). In order to correlate the diode current asymmetricity with the bottom electrode (*i.e.*, CNTs) work function we deposited Al_2O_3 on the two CNT samples followed by Ca top metal electrode. Figure 6 (b) clearly indicates that the asymmetry in the current for a given applied bias is higher in the case of the devices that incorporated higher work function CNTs. These results were reproducible on several devices (not shown here). Additionally, we analyzed these samples in the SEM and the CNTs that were grown on low resistivity substrates were more entangled in comparison to the CNTs that were grown on medium resistivity substrates. The measured *I-V* characteristics indeed are in good agreement with our potential energy level diagram forming a rectifying barrier between the two metals. The higher work function difference between the two electrodes reduces the effective barrier height in the forward bias conditions.

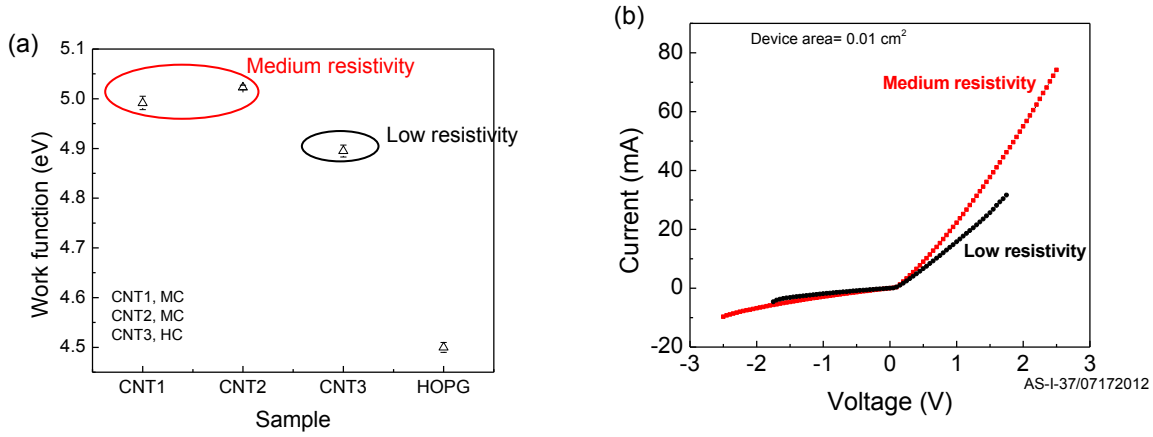

Figure 6. (a) Work function of the CNT's grown on medium resistivity, and low resistivity Si substrates, (b) current-voltage (I-V) characteristics of the devices fabricated using the respective CNT's as bottom electrode in CNT-O-M diodes.

In order to further elucidate and understand the noticeable differences in the rectifying behavior or the asymmetry of the diode due to the behavior of the CNT bottom electrodes in the CNT-O-M diodes, our recent considerations are towards more well aligned CNTs rather than random or entangled CNTs. We have observed a noticeable difference in the diode performance when a different combination of the metal layer is used with the same catalyst. CNTs that were

grown using Ti/Ni/Al/Fe (30/150/10/3 nm) combination produced better rectifying behavior or asymmetry (see Figure 7) even when Al was used as top electrode metal. These results show that there is tremendous potential for CNT-O-M vertical arrays to be further explored for efficient optical rectenna devices.

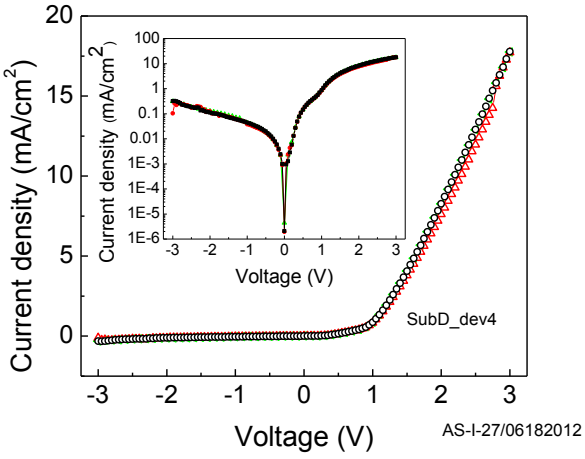

Figure 7. Current density-voltage (*J-V*) characteristics of CNT-O-M (CNT/8 nm Al_2O_3/Al) rectifying diodes (three different devices). CNTs were grown using Ti/Ni/Al/Fe (30/150/10/3 nm) combination of metal layers on medium resistivity Si.

E. Temperature Dependent Current-Voltage Characteristics of the CNT-O-M diodes

We also measured the operational stability of CNT rectenna devices in the temperature range of 5-77 ˚C. The current density-voltage characteristics measured on one device in contact with a temperature-controlled stage are shown in Figure 8. The measurements were carried out on several devices (although not shown here), and the results were consistent from device to device. These results show negligible changes in the electrical performance of these diodes in the temperature range of 5-77 ˚C.

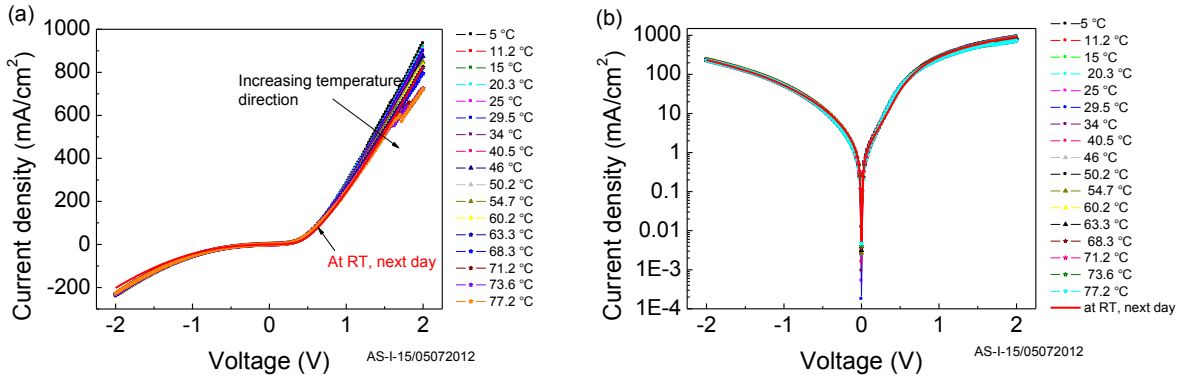

Figure 8. (a) Temperature dependent current density-voltage (*J-V*) characteristics of CNT-O-M (CNT/8 nm Al_2O_3/Al) rectifying diodes, (b) shows the semi logarithmic plot of the data shown in (a).

F. Capacitance Measurements of CNT-O-M Device Structure

Because the asymmetry in these CNT-O-M diodes is also dependent upon the relative dielectric constant of the oxide, we also measured the capacitance characteristics of the CNT-O-M diodes assuming a parallel plate capacitor geometry. The capacitance measured using 340 mV_{rms} as a function of frequencies is shown in Figure 9 (a). The capacitance density calculated under an assumption of a planar configuration generally showed a capacitance density in the range of 30-50 nF/cm^2, and was stable in the MHz ranges. Furthermore, the capacitance as a function of applied DC bias at 100 kHz (shown in Figure 9 (b)) show a near constant value in a wide range of voltages. We note that because capacitors in parallel add, the capacitance of an individual CNT diode junction is substantially less than capacitance density estimated using the planar configuration.

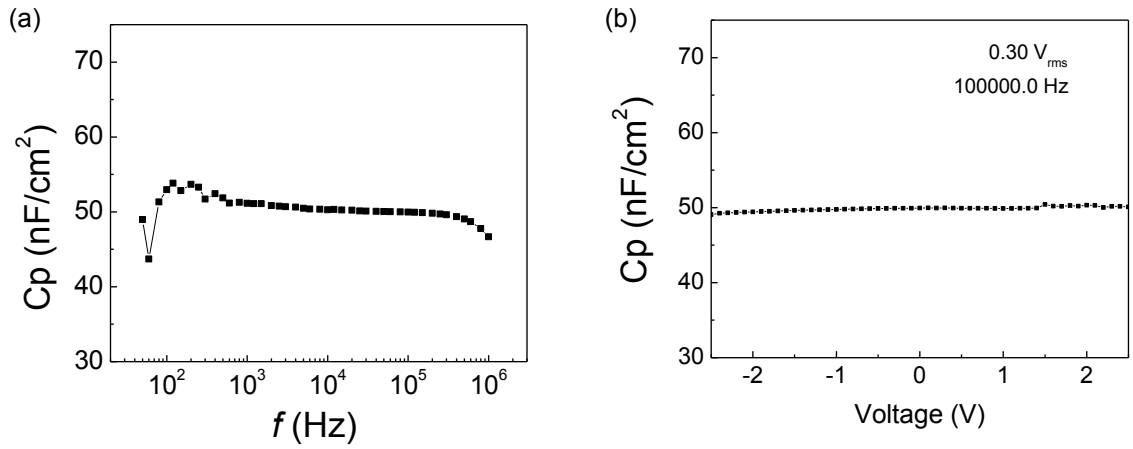

Figure 9. (a) CNT-oxide-metal diode capacitance as a function of frequency, and (b) CNT-oxide-metal diode capacitance as a function of voltage at 100 kHz.

G. *Measurements of CNT-O-M Device Structure under Microscope light*

Figure 10 shows the response of a CNT-O-M diode with a Ca/Al (10 nm/20 nm) semitransparent top metal contact when exposed to illumination by light from a standard microscope. This response was typical of that exhibited by many tested devices. The light illumination was oriented such that the light was incident orthogonal to the surface of the CNT rectenna devices. Exposure to microscope light increased the non-linear response of the diode and lowered the diode curve such that non-zero current was produced at zero applied bias. This can be seen clearly in Figure 10 (b) where the zoomed in view of the curves is presented. These results suggest that the CNT rectenna array is capable of producing power from the microscope light. To further investigate this phenomenon, the zero bias current of the devices was measured as a function of time under microscope illumination. The microscope was turned on at full intensity at a point in time. Then the power of the microscope was gradually reduced until it was completely off. Figure 11 (a) shows the measured zero bias current response. The microscope light is turned on at 150 seconds, and a peak in the current is produced instantaneously! The noise to signal level is high due to the relatively low magnitude of the current. However, it is clear that current is being produced under microscope illumination because of the upward shift in the entire curve when the microscope is on. The broadening of the current response when a

black cover is removed from the sample exposing it to ambient light appears to result from system noise and not any fundamental rectenna process. Figure 11 (b) shows the current response in a control test without the sample. Notice that the signal broadens when the microscope is turned on due an increase in noise. These results provide evidence that the CNT rectenna device demonstrates quantum mechanical tunneling and high frequency rectenna coupling because the energy of the microscope is not high enough to produce heating or photon excitation effects.

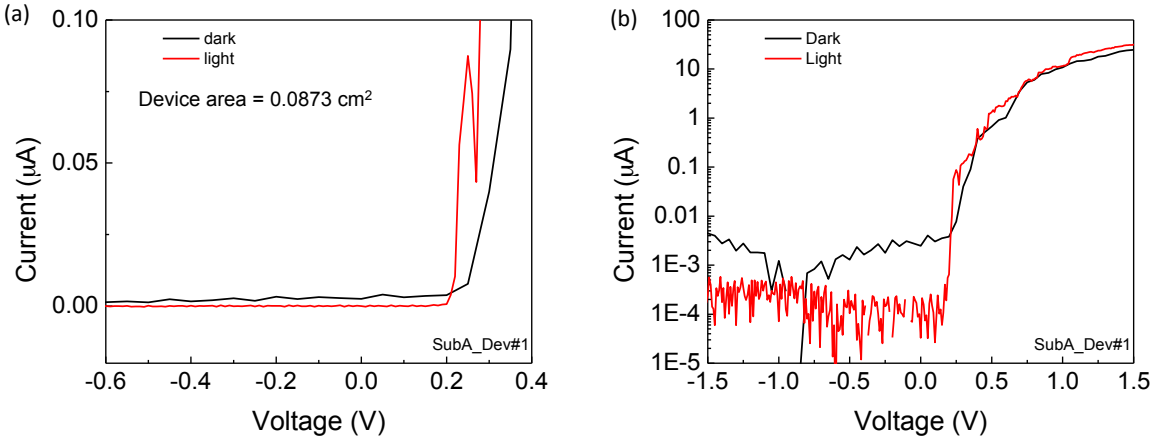

Figure 10. (a) CNT-oxide-metal rectenna exposed to illumination by a microscope light, and (b) the same *I-V* curve plotted on a different scale to show clearly the difference between the dark and light *I-V* response.

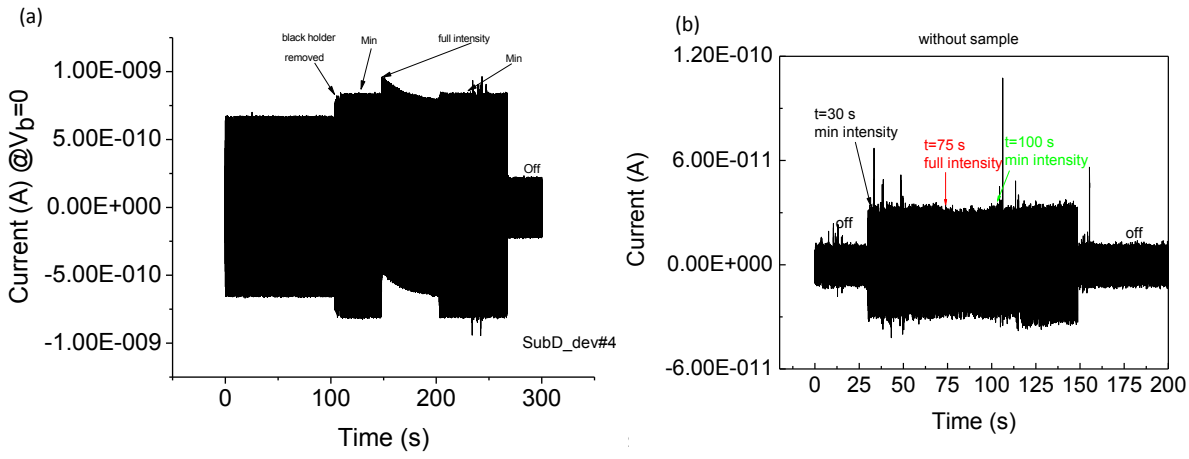

Figure 11. (a) zero bias current response of a CNT-oxide-metal rectenna exposed to illumination by a microscope light, and (b) the current response of the testing system exposed to illumination by the microscope light without the sample. Device area = 0.0873 cm^2.

H. Measurements of CNT-O-M Device Structure under Simulated Solar Illumination

Several CNT rectenna devices were tested under exposure to 1000 W/m^2 AM1.5 illumination from a solar simulator. The solar illumination was oriented such that the light was incident orthogonal to the surface of the CNT rectenna devices. The top metal electrode was the same as the one used above for microscope measurements. The transmissivity of the top metal electrode is estimated from literature to be about 10% on average for the solar spectrum used in our tests. The shift in the *I-V* curves under solar illumination demonstrates that the CNT rectenna device operates as a photodetector at room temperature (see Figure 12). The plot shown in Figure 12 (c) demonstrates that there is energy harvesting in the device as well. The area between the abscissa, ordinate and the light-on line in the fourth quadrant gives the amount of power harvested from the solar source, as is the case with power harvesting estimates for solar cells based on semiconductors.

The zero-bias current, and zero-current voltage in response to the solar illumination was measured as a function of time to further confirm solar power generation with the CNT rectenna devices (Figure 13). The lag of about 100 seconds in both the current and voltage response (*i.e.*, the lack of instantaneous response as was observed in Figure 11 (a)) is due to

the slow response time of the system used for these measurements, which was different than the system used to collect data under microscope illumination where an instantaneous current response to the light was observed. Future work will focus on conducting test under solar illumination with equipment that has a faster response time. The maximum voltages and currents produced under solar illumination were consistently larger than the voltages and currents achieved under illumination by microscope light, which is consistent with theoretical expectations of increased power output with increased illumination intensity; however, other effects such as a shift in the wavelength of peak emission under solar illumination must be consider. Furthermore, the magnitude of the open circuit voltage under solar illumination, approximately 1 mV, is in good agreement with expectations based on the theory of rectenna coupling to electromagnetic energy [1]. Using the maximum open circuit voltage (1 mV) and the maximum short circuit current (1.2 mA/m^2) shown in Figure 13, we estimate that the prototype devices produced around 1 $\mu W/m^2$ of power. This corresponds to an energy conversion efficiency of about 10^{-7} percent for these prototype CNT rectenna devices. This efficiency is by no means the limit of this technology. It is important to note that the CNTs have relatively uniform lengths so they are not expected to couple with equal efficiency to all wavelengths in the solar spectrum. However, the efficiency calculated here is based on an input power that includes the energy in all wavelengths in the solar spectrum. An efficiency based on a coherent input power where the wavelength is matched to the length of the CNT antenna would be significantly, possibly orders of magnitude higher.

The existence and quantification of power generation by CNT rectennas demonstrated here teaches that our approach could be further developed to enable a new age of solar energy conversion, and "all frequency" electromagnetic energy detection, using device structures with no theoretical limit on their obtainable conversion efficiencies.

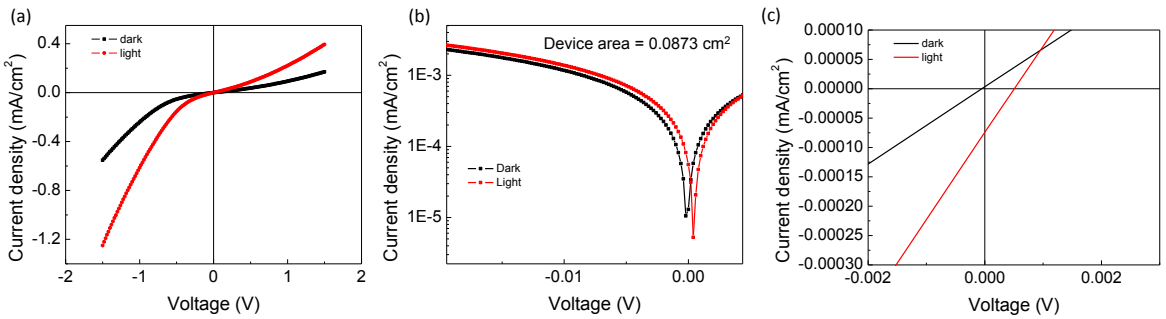

Figure 12. CNT-oxide-metal rectenna exposed to illumination by a solar simulator. (a) I-V cure of light and dark response. The polarity of the connections was reversed in this test. (b) Log-linear plot of the current-voltage response of the CNT rectenna. (c) Magnified view of the I-V response in part (a).

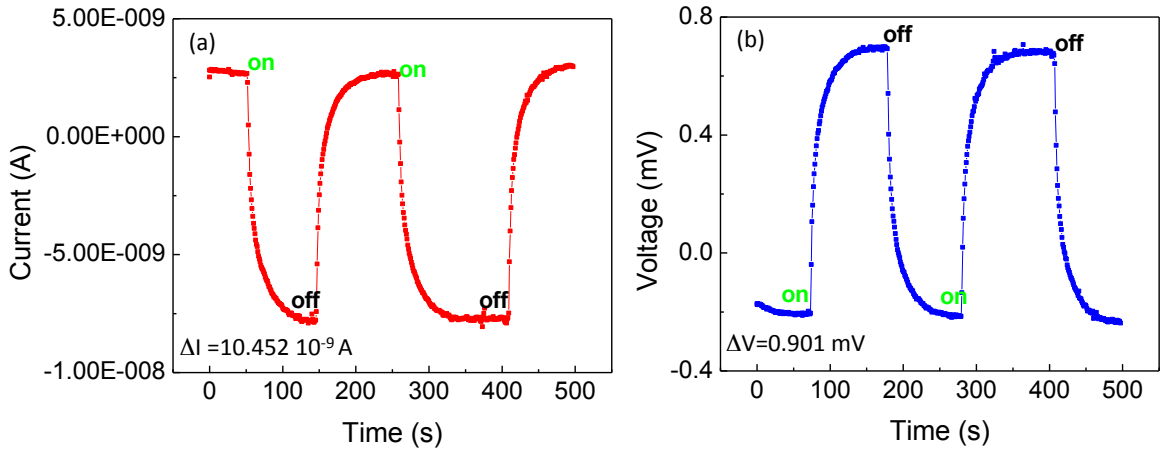

Figure 13. CNT-oxide-metal rectenna exposed to illumination by a solar simulator. (a) Transient current response of the CNT rectenna at zero bias. (b) Transient voltage response of the CNT rectenna at zero current. Device area = 0.0873 cm^2.

Conclusions

This program has produced the first clear quantification of rectenna solar energy conversion in a scalable device structure. Several challenges were met and overcome to reach this end. However, many additional challenges remain that must be addressed to achieve energy conversion efficiencies that make the devices economically competitive for solar and detection applications in the military and commercial sectors. Additional work is also required to elucidate the fundamental quantum mechanical tunneling that underpins rectenna operation. The

nature of the antenna coupling efficiency and the diode resistance in the design develop here also requires further investigation so that these values can be optimized. Circuit optimization was not studied here and is another important area for further investigation. Beyond the aforementioned areas, several other areas of the device design and fundamental operation require extended study. The promise of CNT rectenna devices is clear based on the results of this program; yet much more work is required to realize the full potential of these devices.

References

1. A. Sanchez, C. F. Davis, K. C. Lui Jr., and A. Javan, "The MOM tunneling diode: Theoretical estimate of its performance at microwave and infrared frequencies," *Journal of Applied Physics*, vol. 49(10), pp. 5270-5277, 1978.
2. W. Brown, "The history of power transmission by radio waves," *IEEE Transactions on Microwave Theory and Techniques*, vol. MIT-32(9), pp. 1230-1242, 1984.
3. D. K. Kotter, S. D. Novack, W. D. Slafer, and P. Pinhero, "Solar nantenna electromagnetic collectors," *Proceedings of 2nd ASME International Conference on Energy Sustainability*, ES 2008-54016, 2008.
4. M. R. Osgood III, B. R. Kimball, J. Carlson, "Nanoantenna-coupled MIM nanodiodes for efficient vis/nir energy conversion," *Proceedings of SPIE*, vol. 6652, 665203, 2007.
5. B. Berland, "Photovoltaic technologies beyond the horizon: Optical rectenna solar cell," National Renewable Energy Laboratory Report, NREL/SR-520-33263, 2003.
6. K. Kempa, J. Rybczynski, Z. Huang, K. Gregorczyk, A. Vidan, B. Kimball, J. Carlson, G. Benham, Y. Wang, A. Herczynski, and Z. Ren, "Carbon nanotubes as optical antennae," *Advanced Materials*, vol. 19, pp. 421-426, 2007.
7. R. Stratton, "Volt-current characteristics for tunneling through insulating films," *Journal of Physics and Chemistry of Solids*, vol. 23, pp. 1177-1190, 1962.